



Brookhaven
National Laboratory

BNL-101870-2014-TECH

AD/RHIC/RD/87;BNL-101870-2013-IR

RHIC Dipole End Volume Weld Evaluation

S. Kane

March 1995

Collider Accelerator Department
Brookhaven National Laboratory

U.S. Department of Energy

USDOE Office of Science (SC), Nuclear Physics (NP) (SC-26)

Notice: This technical note has been authored by employees of Brookhaven Science Associates, LLC under Contract No. DE-AC02-76CH00016 with the U.S. Department of Energy. The publisher by accepting the technical note for publication acknowledges that the United States Government retains a non-exclusive, paid-up, irrevocable, world-wide license to publish or reproduce the published form of this technical note, or allow others to do so, for United States Government purposes.

DISCLAIMER

This report was prepared as an account of work sponsored by an agency of the United States Government. Neither the United States Government nor any agency thereof, nor any of their employees, nor any of their contractors, subcontractors, or their employees, makes any warranty, express or implied, or assumes any legal liability or responsibility for the accuracy, completeness, or any third party's use or the results of such use of any information, apparatus, product, or process disclosed, or represents that its use would not infringe privately owned rights. Reference herein to any specific commercial product, process, or service by trade name, trademark, manufacturer, or otherwise, does not necessarily constitute or imply its endorsement, recommendation, or favoring by the United States Government or any agency thereof or its contractors or subcontractors. The views and opinions of authors expressed herein do not necessarily state or reflect those of the United States Government or any agency thereof.

AD/RHIC/RD-87
REVISED

RHIC PROJECT
Brookhaven National Laboratory

RHIC Dipole End Volume Weld Evaluation

S. Kane, A. Farland, M. Anerella

May 1995

RHIC Dipole End Volume Weld Evaluation

S. Kane, A. Farland, M. Anerella

Abstract

The End Volume weld on the RHIC Dipole Magnet is a fillet weld attaching a cylindrical shell to flat, circular end plates to form a volume within which magnet electrical connections are located. These welds were found undersized on the first 48 magnets manufactured by Grumman. Subsequent inspection found the welds undersized as much as 3/32" for a specified 3/8" x 1/2" inch fillet. The weld contour also changes with its location around the periphery. A test sample was welded using the identical process for delivered magnets. The test sample was instrumented using dial indicators, then hydraulically pressurized in conformance with the American Society of Mechanical Engineers (ASME) Boiler & Pressure Vessel Code. Testing was discontinued at 2,000 psi without failure. The test data shows the non-conforming weld meets ASME Boiler & Pressure Vessel Code requirements for a design pressure of 275 psi.

Background

The RHIC Dipole Magnet Coldmass has a 14.25" outside diameter volume installed on each end. This volume provides the room necessary for magnet electrical components, such as diodes, lead connections, and lead expansion joints. The volume is formed by a cylindrical shell, 0.375" thick, which increases to 0.425" thick at the ends for attachment to the 1.00" thick flat plate (coldmass yoke containment end plate) which forms the inner head of the volume, and the 1.50" thick flat plate which forms the outer head of the volume. The cylinder is welded to the heads using 3/8" x 1/2" fillet welds. Although this attachment does not conform to the permitted joint designs in American Society of Mechanical Engineers (ASME) Boiler and Pressure Vessel Code, the stresses in the joint are below those permitted by Division 2, Alternate Rules, of Section VIII, Rules of Construction of Pressure Vessels. This joint was used to facilitate detachment of the end volume for magnet electrical repairs while preserving the end volume components for reattachment.

The outer head and cylinder are welded by a Grumman subcontractor, and are full fillet welds. This subassembly is then attached to the magnet coldmass yoke containment end plate by Grumman using an orbital welder. Inspection of this weld at the 12 o'clock position shows a full fillet of proper geometry. However, further inspection around the periphery reveals distorted weld contours, as shown in Figure 1. Measurement of this weld reveals the axial leg was less than 0.5", and as little as 0.4".

Several delivered magnets were inspected by E. Jochen, Central Shops Weld Inspector, using a custom 3/8" x 1/2" fillet weld gage, especially manufactured by Central Shops. The

measurements are listed in Appendix A. Additional gages were manufactured by Central Shops and provided to Grumman for their in-house inspection. The non-conforming welds were corrected by magnet serial numbers DRG-131 and DRG-519 (magnet sequence number 49).

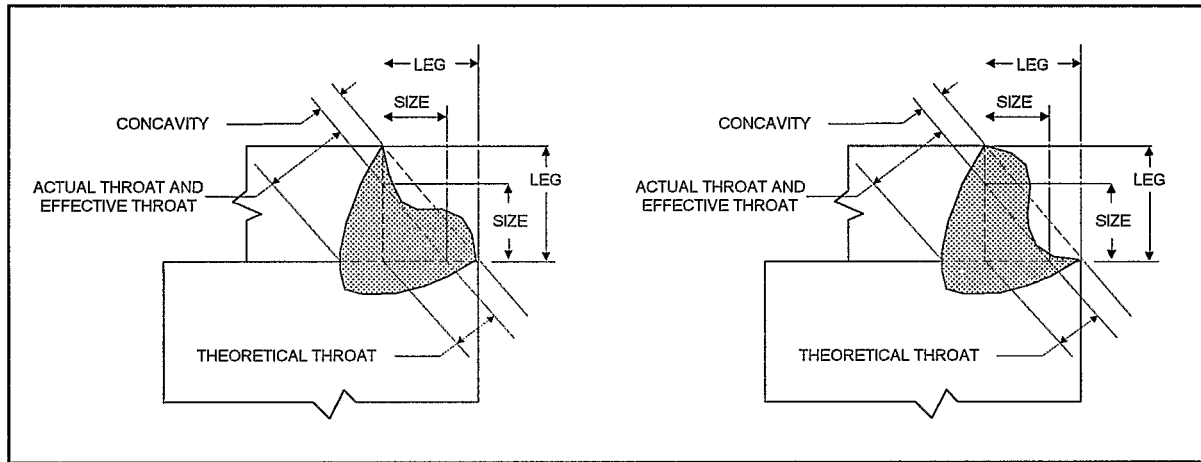


Figure 1. Typical Grumman End Volume Weld Profiles

The issue to be addressed became the acceptability of the non-conforming welds on the delivered magnets. The ASME Boiler & Pressure Vessel Code provides empirical methods to establish allowable pressure. Specifically, Section VIII, Division 1, *Rules for Construction of Pressure Vessels*, Paragraph UG-101, Proof Tests to Establish Maximum Allowable Working Pressure, provides two types of tests to determine the internal maximum allowable working pressure — tests based upon material yielding and tests based upon bursting of the part. The tests based upon material yielding are prescribed by paragraphs UG-101(l), (n), and (o). These are:

- UG-101(l) Brittle-Coating Test Procedure - the parts to be tested are coated with a brittle coating. Pressure is applied and released incrementally, until the coating begins flaking or strain lines appear.
- UG-101(n) Strain Measurement Test Procedure - strain gages are attached at the most highly stressed location of the part. Pressure is applied and released incrementally, until the strains reach 0.2% permanent strain.
- UG-101(o) Displacement Measurement Test Procedure - devices capable of measuring to 0.001 inches shall be used to measure displacement at the most highly stressed location. Pressure is applied and released incrementally, until the plot of displacement under pressure deviates from a straight line.

Maximum allowable working pressure is then calculated by

$$P = 0.5 \times H \times \frac{S_y}{S_{y\text{avg}}} \quad \text{or} \quad P = 0.4 \times H$$

where

- H = hydrostatic test pressure when test was stopped
- S_y = specified minimum yield strength
- S_{y avg} = average actual yield strength

The second formula is used if the actual average yield strength is not determined by test specimens.

The test based upon bursting of the part is prescribed by UG-101(m). Hydrostatic pressure is increased until the part bursts. Maximum allowable working pressure is then calculated by

$$P = \frac{B}{5} \times \frac{S_{\mu} E}{S_{\mu \text{ avg}}} \quad \text{or} \quad P = \frac{B}{5} \times \frac{S_{\mu} E}{S_{\mu r}}$$

where

- B = bursting test pressure
- E = weld joint efficiency
- S_μ = specified minimum tensile strength
- S_{μ avg} = average actual tensile strength
- S_r = maximum actual tensile strength of range of specification

Procedure

A proof test of an article representing the identical weld configuration for the delivered magnets would address all non-conforming magnets. A test specimen was prepared using an actual dipole end volume shell and a 1.25" thick plate machined to the drawing diameter. These were welded by Grumman using the RHIC-specific weld alloy, RHIC-MAG-M-4360, and the identical welding machine, following the procedure used to manufacture the non-conforming welds. A head was designed following ASME Code Rules and manufactured by Brookhaven National Laboratory Central Shops. This design, shown in Figure 2, employs a butt weld, which was performed by the Brookhaven National Laboratory Weld Shop. A hole was bored through the Code head and threaded to accept a 1/2" Swage-Lok fitting.

The fillet-welded head was instrumented using five Starrett dial indicators with 0.001" increments to measure the displacement at the center and the periphery of the head. These measurements were referenced by a sixth dial indicator installed at the base of the test article. The test article was held in a lamination tray to catch any oil if the article burst during testing. A Teledyne-Sprague Engineering Model S-216-C-150 pneumatic-actuated hydraulic pump with a 16,000 psi capacity was connected to the test article using a flexible hose. Two gauges were used to measure the test pressure; one with a maximum reading of 3,000 psi at 25 psi increments, the other with a maximum reading of 10,000 psi at 500 psi increments. Valving permitted isolation of the 3,000 psi gauge if pressures above its maximum capacity were necessary.

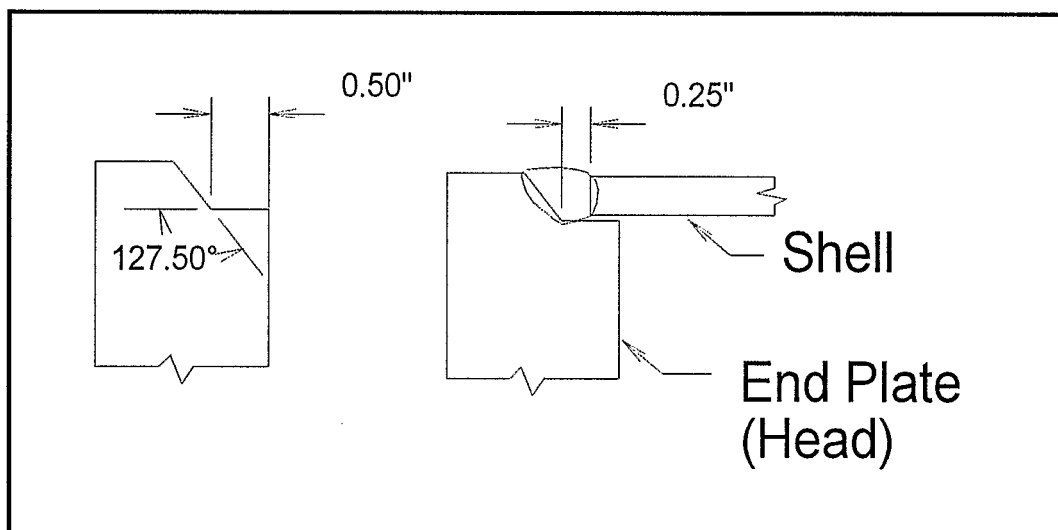


Figure 2. Test Article Code Joint Detail

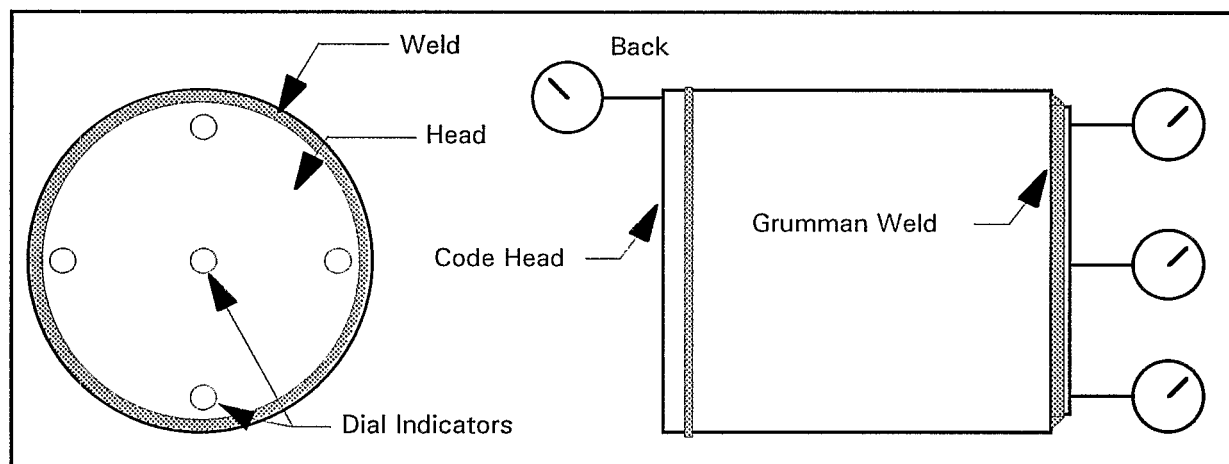


Figure 3. Dial Indicator Location

The ultimate objective of the test was to burst the part. However, instrumentation was applied to capture data for evaluation using the displacement test method. The dial indicators were zeroed immediately preceding the test. The general procedure followed was to apply pressure, record dial indicator readings, then release the pressure and, again, record dial indicator readings. The initial pressure was the design pressure, 275 psi. The next pressure level was 500 psi, and subsequent pressure levels were increased in 250 psi increments, until 1,250 psi. The center dial indicator showed 0.182" displacement at 1,250 psi. To avoid excessive strain rates, the next pressure level was 1,400 psi, and subsequent pressure levels were increased in increments of 200 psi. The fitting on the test article began leaking, and the test was stopped after 2,000 psi to tighten the fitting. However, this did not stop the leakage. While attempting the 2,200 psi pressure level, leakage prevented achieving a pressure beyond 2,000 psi. The test was stopped at this point, without having burst the part. However, the 6 o'clock dial indicator developed a "heart beat" synchronized with the pump. This was caused by continuous yielding of the material at that location under pressure during the pump pressure stroke, causing increased displacement

measured by the 6 o'clock dial indicator. At the end of the pressure stroke, the pressure would bleed down to 2,000 psi before the next pressure stroke, during which the displacement measured by the 6 o'clock dial indicator would decrease. The data collected is tabulated in Appendix B.

Results and Discussion

Testing on the Dipole Coldmass Patches¹ found the displacement test method yielded a maximum allowable working pressure close to, but less than, the strain measurement test method. The size of this test article would provide greater accuracy using the displacement measurement method. Mathematical modeling of the stresses and strains in the test article head is limited to lower pressures by the elastic limits of the material. Using conventional formulae for a 1.25" thick circular flat plate, and assuming fixed end conditions, the greatest stresses are located at the welds. The stress at the weld at 275 psi is 5,926 psi, and the shear reaction is 921 lbs/in. However, unlike the test specimen, the coldmass yoke containment end plate contains a 2.912" diameter hole in the middle, and is welded to the coldmass shells at a diameter of 10.86". The inner and outer boundaries are restrained by the welds, and the pressure is only applied to the area of the plate bounded by those inner and outer boundaries. The thickness of the pressure-bearing portion of the plate is 1.00". The stress at the welds for the actual design configuration at 275 psi is just 1,035 psi with a shear reaction of 357 lbs/in. Therefore, the test configuration applies stresses 473% greater than the stresses for the actual configuration, and shear reactions are 158% greater than the actual configuration. The calculations for the models are provided in Appendix C. Disregarding the differences between the actual and test stresses would, therefore, be conservative.

Evaluation of Results using Displacement Measurement Method

The dial indicator indexing the test head was located at the center. Both models for this test show the center of the head will experience the greatest displacement, satisfying the requirement of UG-101(o), Displacement Measurement Test Procedure, subparagraph (1), for location of the indicators. UG-101(o), Displacement Measurement Test Procedure, subparagraph (3) requires two curves of the displacement versus the test pressure be plotted for each reference point — one plot is of the displacement under pressure, the other shows permanent displacement when pressure is removed. Pressure is applied and released incrementally, until the plot of displacement under pressure deviates from a straight line. These plots are shown in Figure 4.

The plot of displacement under pressure departs from a straight line beyond 1,000 psi. This is verified by the plot of displacement after pressure, shown as Zero, which also departs from a straight line after 1,000 psi. The maximum allowable working pressure is defined by:

$$P = 0.4 \times H$$

¹ S. Kane, A. Farland, M. Anerella, *RHIC Dipole Coldmass Patch Weld Evaluation*, Project Tech Note AD/RHIC/RD-86, March 1995

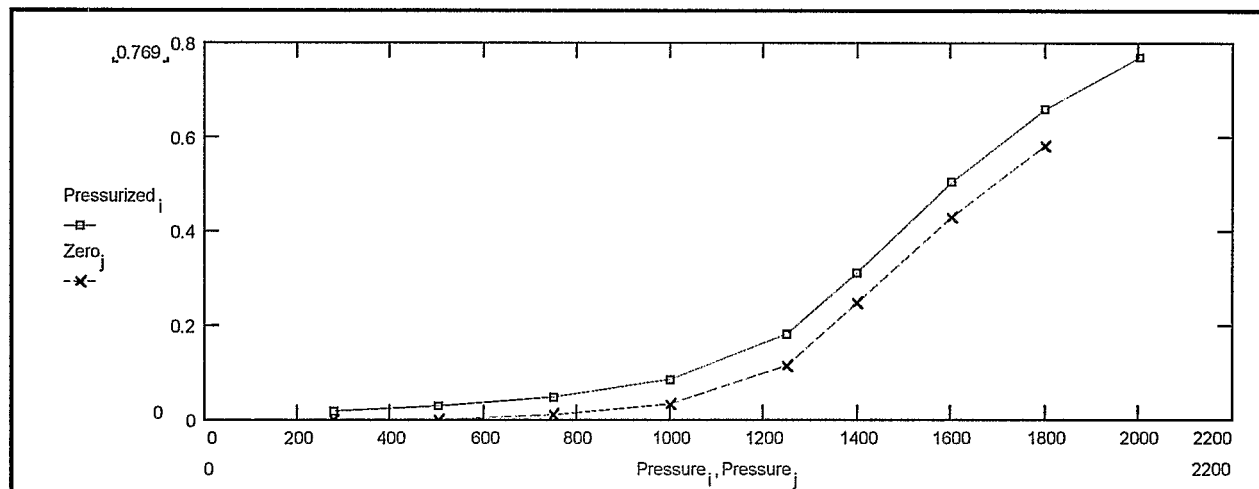


Figure 4. Displacement Data Plot

Thus the maximum allowable working pressure for the end volume weld using the ASME Displacement Measurement Test Procedure of UG-101, Proof Tests to Establish Maximum Allowable Working Pressure, is 400 psi.

Assessment of the Test Results

The displacement test method was previously shown to produce conservative results. The mathematical model comparing the stresses at the welds in the test article to the stresses in the welds for the actual design shows the test article produces stresses much greater than the actual design stresses. Ignoring this conservatism, the ASME maximum allowable working pressure resulting from the proof test is 400 psi, and exceeds the RHIC Cryogenic System design pressure of 275 psi.

The disparity in the test results may cause speculation about “over design.” The ASME requirements use the yield strength as the criterion for material limits. This is sufficiently true for most engineering materials. However, material characteristics, hence their analytical techniques, are not predictable beyond the proportional limit of their yield strengths. For this case, where Type 304 austenitic stainless steels are used, their yield strengths are just 30,000 psi, compared with their ultimate strengths of 75,000, for a ratio of 1:2.5. Few other practical engineering materials for pressure vessels have this characteristic. Thus, the rules are designed to accommodate the majority of materials used, while erring on the side of conservatism for other materials. The ASME recognizes these issues, and provides other methods, such as the proof test used here, to determine a component’s safe maximum allowable working pressure.

Additionally, the ASME requirements use the minimum specified yield strength as the benchmark for material limits. These limits are derived from the worst case yield strengths within the material’s specified chemical composition range. In practice, these materials exceed these values by at least 10%. Finally, the RHIC-specific weld alloy, RHIC-MAG-M-4360, is a new generation

of cryogenic pressure vessel superalloys. While developed primarily for superior notch toughness at 4°K, it possesses superior yield strength. BNL testing shows its room temperature yield strength to be between 44 and 50 ksi — as much as 67% greater than the base material minimum specified yield strength. The success of this proof test is attributed to the exceptional properties of this weld alloy and not “over design.”

Conclusions

The Grumman Dipole coldmass yoke containment end plate-to-end volume outer diameter fillet welds with their variable and non-conforming profile satisfy the requirements of the ASME Boiler & Pressure Vessel Code for the RHIC design maximum allowable working pressure of 275 psi.

APPENDIX A

RHIC Grumman Dipole

Coldmass Yoke Containment End Plate-to-End Volume Fillet Weld Size

RHIC Grumman Dipole
Coldmass Yoke Containment End Plate-to-End Volume Fillet Weld Size

Magnet Serial No.	Lead End	Non-Lead End
DRG 117	- 1/16"	- 1/16"
DRG 119	- 1/16"	- 1/16"
DRG 120	- 1/16" - 3/32"	- 1/16"
DRG 121	- 1/16" - 3/32"	- 1/16"
DRG 123	- 1/16"	- 1/16"
DRG 124	- 1/16"	- 1/16"
DRG 128	- 1/16"	- 1/16"
DRG 129	- 1/16"	- 1/16"
DRG 130	- 1/16"	- 1/16"
DRG 503	- 1/16"	- 1/16"
DRG 504	- 1/16" - 3/32"	- 1/16" - 3/32"
DRG 505	- 1/16" - 3/32"	- 1/16" - 3/32"

APPENDIX B

RHIC Grumman Dipole

Coldmass Yoke Containment End Plate-to-End Volume Fillet Weld

Proof Test Data

RHIC Grumman Dipole
Coldmass Yoke Containment End Plate-to-End Volume Fillet Weld
Proof Test Data

Pressure (psi)	Center	12 O'Clock	3 O'Clock	6 O'Clock	9 O'Clock	Back
0	.000	.000	.000	.000	.000	.000
275	.019	.003	.003	.003	.003	.0005
0	.000	.000	.000	.000	.000	.000
500	.030	.006	.005	.005	.005	.0005
0	.0015	.00025	.000	.000	.000	.000
750	.0495	.00925	.0075	.00775	.00725	.001
0	.0095	.00125	.001	.001	.001	.000
1000	.086	.015	.0125	.0125	.01225	.002
0	.033	.00525	.0125	.003	.003	.001
1250	.182	.030	.025	.025	.025	.0025
0	.116	.017	.0255	.0135	.01325	.0015
1400	.310	.050	.044	.043	.042	.0035
0	.248	.037	.0405	.030	.030	.002
1600	.504	.079	.069	.069	.068	.005
0	.430	.065	.0555	.055	.054	.003
1800	.660	.103	.089	.090	.087	.007
0	.583	.088	.07675	.076	.07325	.0055
Repositioned Center Gauge	.604	.087	.076	.039	.07275	.0055
2000	.790	.125	.109	.072	.1025	.016

APPENDIX C

RHIC Grumman Dipole

Coldmass Yoke Containment End Plate-to-End Volume Fillet Weld

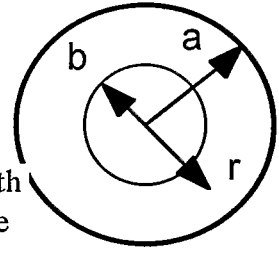
Mathematical Models

Analysis of Dipole End Volume Proof Test

$$v := 0.305 \quad t := 1.00 \cdot \text{in} \quad q := 275 \cdot \text{psi} \quad a := \frac{13.4}{2} \cdot \text{in} \quad b := \frac{10.485}{2} \cdot \text{in} \quad E := 27.6 \cdot 10^6 \cdot \text{psi} \quad r_o := b$$

$$D := \frac{E \cdot t^3}{12 \cdot (1 - \nu^2)} \quad D = 2535902 \cdot \text{lbf} \cdot \text{in}$$

The disk has outer radius 'a' and inner radius 'b'. Functions are measured from the center; 'c' is the center, 'a' is the outer edge, and 'r' is a point in between.



The following equations are from Roark's Table 24, Case 2f., for a circular plate with inner and outer boundaries, outer edge fixed, inner edge guided. This represents the actual loading of the plate in the dipole.

$$C2 := \frac{1}{4} \left[1 - \left[\left(\frac{b}{a} \right)^2 \cdot \left[1 + \left(2 \cdot \ln \left(\frac{a}{b} \right) \right) \right] \right] \right] \quad C5 := \frac{1}{2} \left[1 - \left(\frac{b}{a} \right)^2 \right] \quad C8 := \frac{1}{2} \left[1 + \nu + \left[(1 - \nu) \cdot \left(\frac{b}{a} \right)^2 \right] \right]$$

$$L17 := \frac{1}{4} \left[1 - \left(\frac{1 - \nu}{4} \right) \cdot \left[1 - \left(\frac{r_o}{a} \right)^4 \right] - \left[\left(\frac{r_o}{a} \right)^2 \cdot \left[1 + \left[(1 + \nu) \cdot \ln \left(\frac{a}{r_o} \right) \right] \right] \right] \right] \quad L14 := \frac{1}{16} \left[1 - \left(\frac{r_o}{a} \right)^4 - \left[4 \cdot \left(\frac{r_o}{a} \right)^2 \cdot \ln \left(\frac{a}{r_o} \right) \right] \right]$$

$$L11 := \frac{1}{64} \left[1 + \left[4 \cdot \left(\frac{r_o}{a} \right)^2 \right] - \left[5 \cdot \left(\frac{r_o}{a} \right)^4 \right] - \left[4 \cdot \left(\frac{r_o}{a} \right)^2 \cdot \left[2 + \left(\frac{r_o}{a} \right)^2 \right] \cdot \ln \left(\frac{a}{r_o} \right) \right] \right]$$

$$F2(r) := \frac{1}{4} \left[1 - \left[\left(\frac{b}{r} \right)^2 \cdot \left[1 + \left(2 \cdot \ln \left(\frac{r}{b} \right) \right) \right] \right] \right] \quad G11(r) := \frac{1}{64} \left[1 + \left[4 \cdot \left(\frac{r_o}{r} \right)^2 \right] - \left[5 \cdot \left(\frac{r_o}{r} \right)^4 \right] - \left[4 \cdot \left(\frac{r_o}{r} \right)^2 \cdot \left[2 + \left(\frac{r_o}{r} \right)^2 \right] \cdot \ln \left(\frac{r}{r_o} \right) \right] \right]$$

$$F5(r) := \frac{1}{2} \left[1 - \left(\frac{b}{r} \right)^2 \right] \quad F8(r) := \frac{1}{2} \left[1 + \nu + \left[(1 - \nu) \cdot \left(\frac{b}{r} \right)^2 \right] \right] \quad G14(r) := \frac{1}{16} \left[1 - \left(\frac{r_o}{r} \right)^4 - \left[4 \cdot \left(\frac{r_o}{r} \right)^2 \cdot \ln \left(\frac{r}{r_o} \right) \right] \right]$$

$$G17(r) := \frac{1}{4} \left[1 - \left(\frac{1 - \nu}{4} \right) \cdot \left[1 - \left(\frac{r_o}{r} \right)^4 \right] - \left[\left(\frac{r_o}{r} \right)^2 \cdot \left[1 + \left[(1 + \nu) \cdot \ln \left(\frac{r}{r_o} \right) \right] \right] \right] \right]$$

$$y_b := \frac{-q \cdot a^4}{D} \cdot \left(\frac{C2 \cdot L14}{C5} - L11 \right) \quad Mr_b := \frac{q \cdot a^2 \cdot L14}{C5} \quad Mr_a := -q \cdot a^2 \cdot \left(L17 - \frac{C8}{C5} \cdot L14 \right) \quad Q_a := \frac{-q}{2 \cdot a} \cdot (a^2 - r_o^2)$$

$$C2 = 0.022 \quad C5 = 0.194 \quad C8 = 0.865 \quad L11 = 0.000084701 \quad L14 = 0.002 \quad L17 = 0.021$$

$$Mr_b = 97.073 \cdot \text{lbf} \quad Mr_a = -172.574 \cdot \text{lbf} \quad y_b = -0.00002 \cdot \text{in} \quad Q_a = -357.217 \cdot \frac{\text{lbf}}{\text{in}}$$

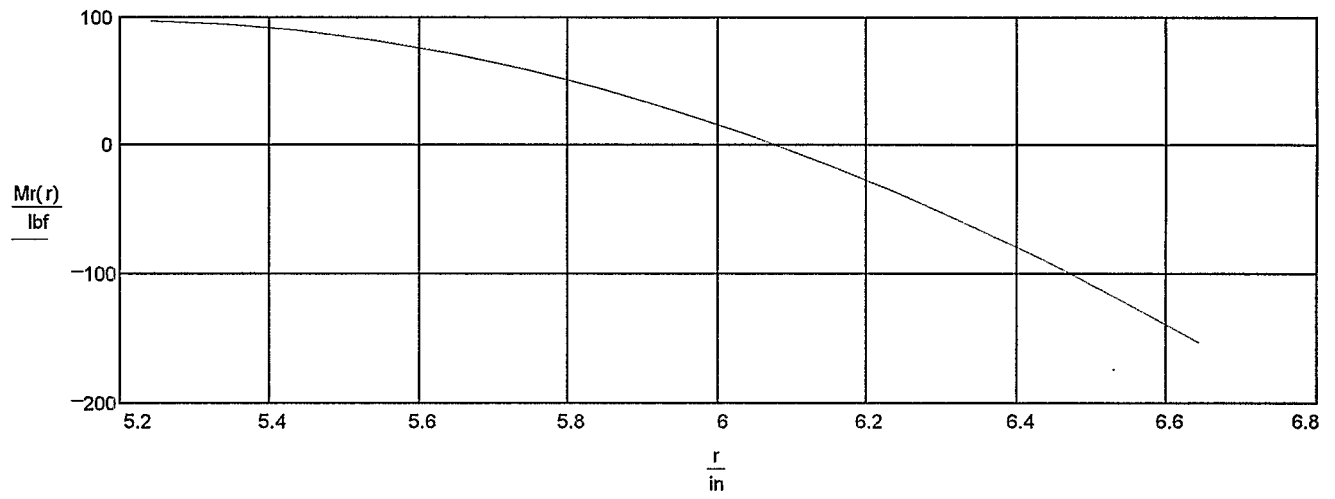
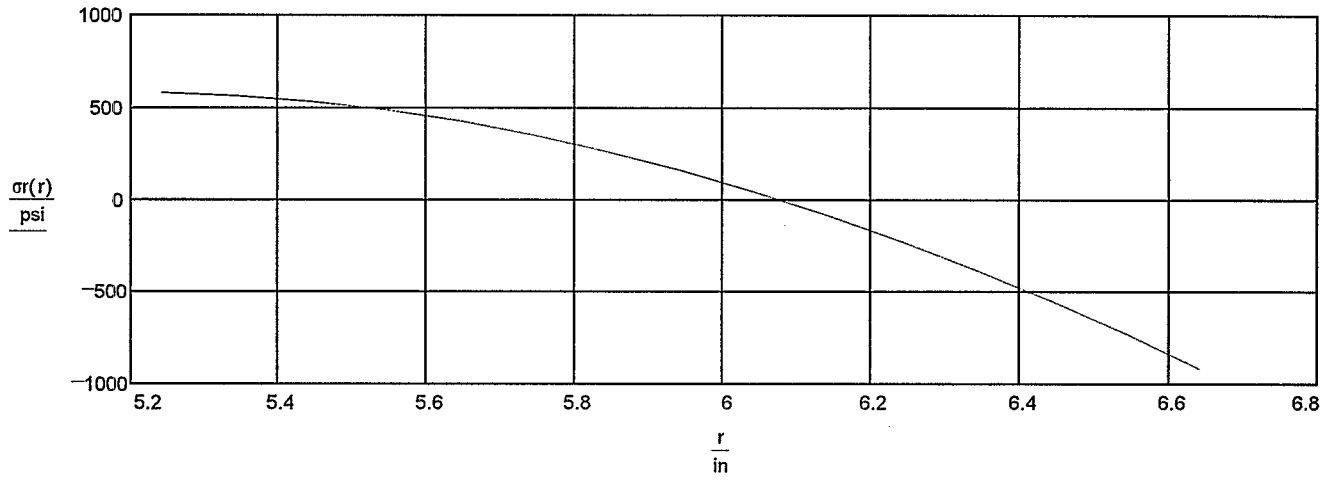
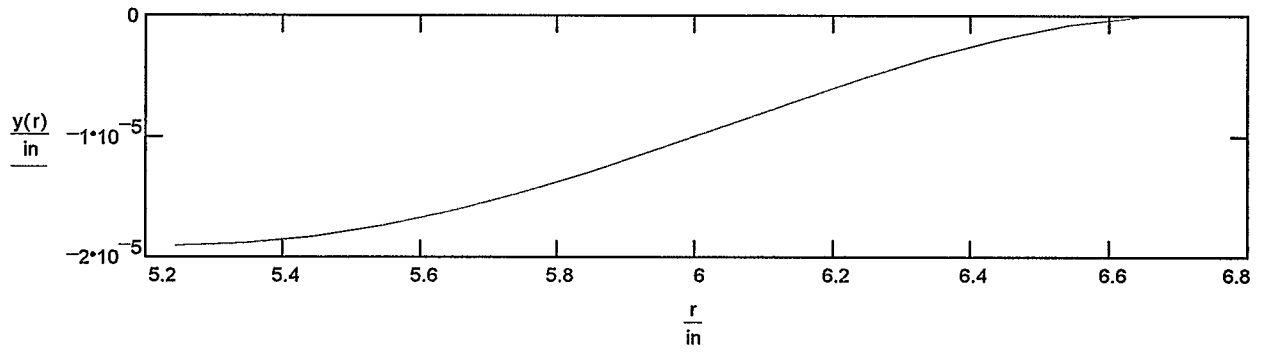
$$y(r) := y_b + Mr_b \cdot \frac{r^2}{D} \cdot F2(r) - q \cdot \frac{r^4}{D} \cdot G11(r) \quad \theta(r) := Mr_b \cdot \frac{r}{D} \cdot F5(r) - q \cdot \frac{r^3}{D} \cdot G14(r)$$

$$Mr(r) := Mr_b \cdot F8(r) - q \cdot r^2 \cdot G17(r) \quad Mt(r) := \frac{\theta(r) \cdot D \cdot (1 - \nu^2)}{r} + \nu \cdot Mr(r) \quad Q(r) := -\frac{q}{2 \cdot r} \cdot (r^2 - r_o^2)$$

$$\sigma_r(r) := \frac{Mr(r) \cdot 6}{t^2} \quad \sigma_t(r) := \frac{Mt(r) \cdot 6}{t^2} \quad \epsilon_r(r) := \frac{\sigma_r(r)}{E} \quad \epsilon_t(r) := \frac{\sigma_t(r)}{E}$$

$$\sigma_r(b) = 582.44 \cdot \text{psi} \quad \sigma_r(a) = -1035.443 \cdot \text{psi} \quad \sigma_t(b) = 177.644 \cdot \text{psi} \quad \sigma_t(a) = -315.81 \cdot \text{psi}$$

$$Q(a) = -357.217 \cdot \frac{\text{lbf}}{\text{in}} \quad Q(b) = 0 \cdot \frac{\text{lbf}}{\text{in}}$$

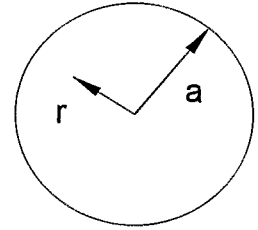


Analysis of Dipole End Volume Proof Test

$\nu := 0.305$ $t := 1.25 \cdot \text{in}$ $q := 275 \cdot \text{psi}$ $a := \frac{13.4}{2} \cdot \text{in}$ $b := \frac{10.485 \cdot \text{in}}{2}$ $r := 0 \cdot \text{in}$ $E := 27.6 \cdot 10^6 \cdot \text{psi}$

$D := \frac{E \cdot t^3}{12 \cdot (1 - \nu^2)}$ $D = 4952934 \cdot \text{lbf} \cdot \text{in}$

The disk has radius 'a'. Functions are measured from the center; 'c' is the center, 'a' is the outer edge, and 'r' is a point in between.



Simply Supported

$yc_{ss} := \frac{-a^4 \cdot (5 + \nu)}{64 \cdot D \cdot (1 + \nu)} \cdot q$ $yc_{ss} = -2.584 \cdot 10^{-5} \cdot \frac{\text{in}}{\text{psi}}$ $yc_{ss}(q) := \frac{-a^4 \cdot (5 + \nu)}{64 \cdot D \cdot (1 + \nu)} \cdot q$ $yc_{ss}(q) = -0.0071 \cdot \text{in}$

$Mc_{ss} := \frac{a^2 \cdot (3 + \nu)}{16} \cdot q$ $Mc_{ss} = 9.3 \cdot \text{in}^2$ $Mc_{ss}(q) := \frac{a^2 \cdot (3 + \nu)}{16} \cdot q$ $Mc_{ss}(q) = 2550 \cdot \text{lbf}$

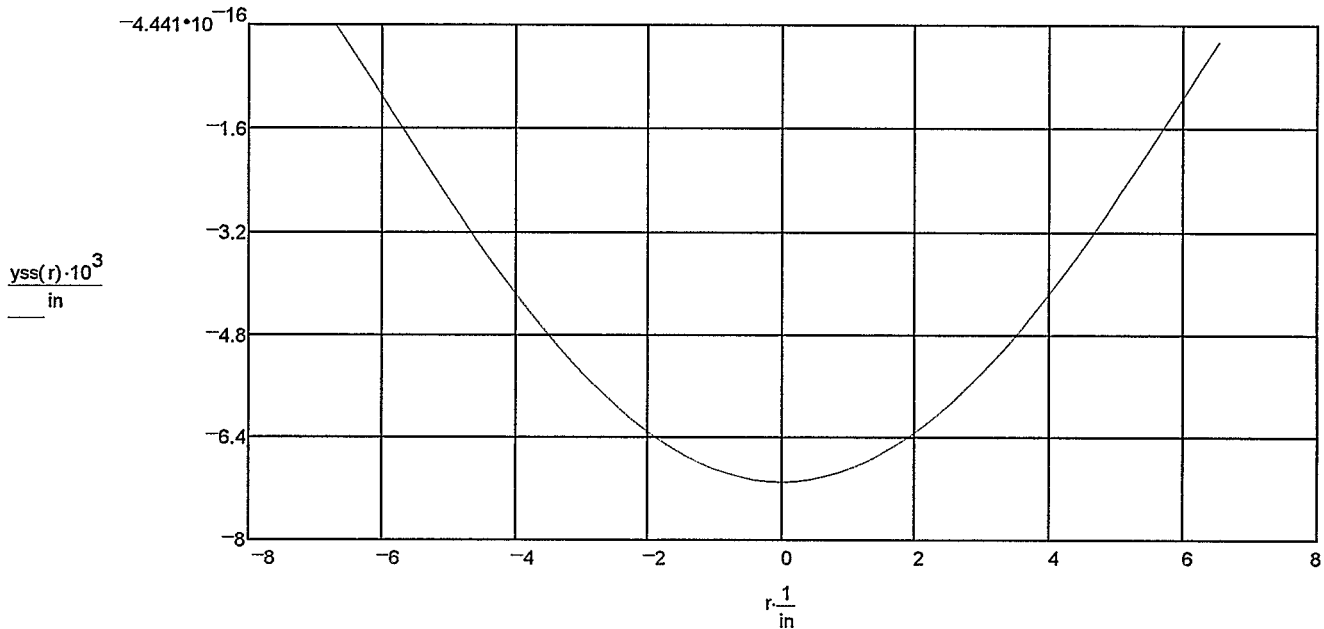
$\theta_{ass} := \frac{a^3}{8 \cdot D \cdot (1 + \nu)} \cdot q$ $\theta_{ass} = 0.0003 \cdot \frac{\text{deg}}{\text{psi}}$ $\theta_{ass}(q) := \frac{a^3}{8 \cdot D \cdot (1 + \nu)} \cdot q$ $\theta_{ass}(q) = 0.1 \cdot \text{deg}$

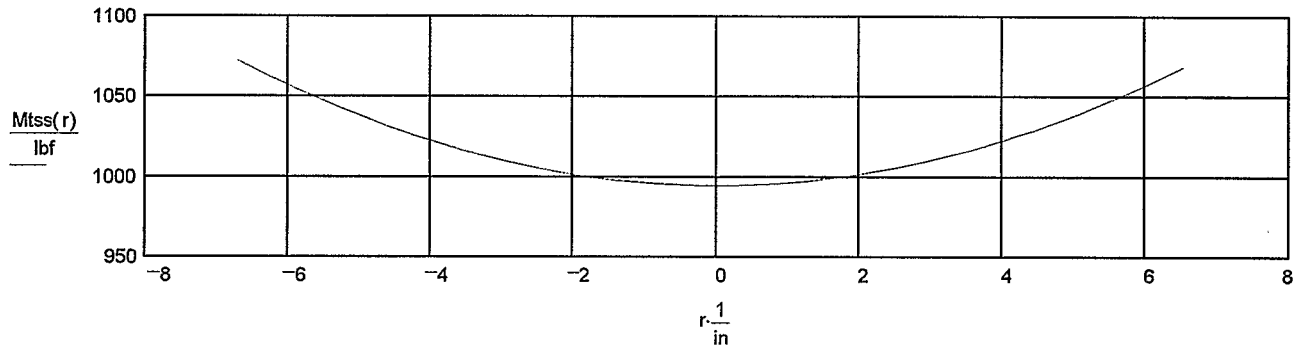
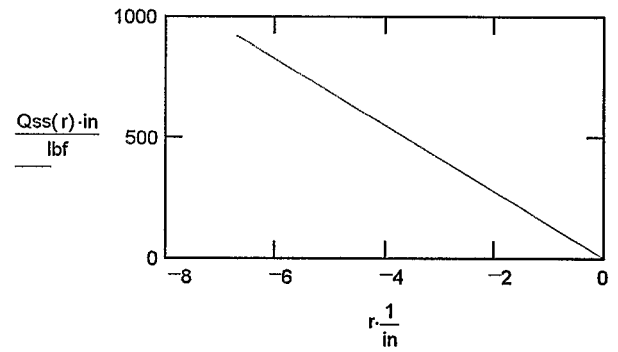
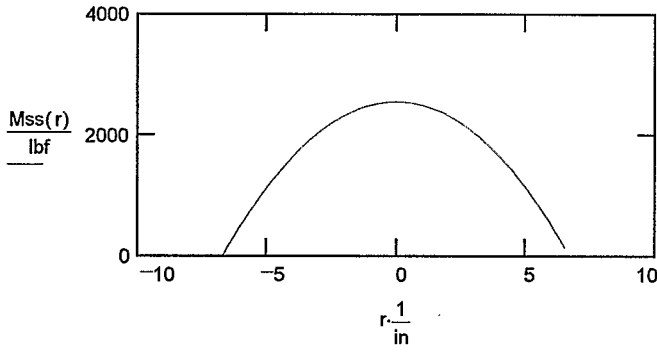
$Q_{ass} := -\frac{a}{2} \cdot q$ $Q_{ass} = -3.35 \cdot \text{in}$ $Q_{ass}(q) := -\frac{a}{2} \cdot q$ $Q_{ass}(q) = -921.25 \cdot \frac{\text{lbf}}{\text{in}}$

$y_{ss}(r) := \left[\frac{-a^4 \cdot (5 + \nu)}{64 \cdot D \cdot (1 + \nu)} + \frac{a^2 \cdot (3 + \nu) \cdot r^2}{32 \cdot D \cdot (1 + \nu)} - \frac{r^4}{64 \cdot D} \right] \cdot q$ $M_{ss}(r) := \frac{q \cdot (3 + \nu)}{16} \cdot (a^2 - r^2)$ $Q_{ss}(r) := \frac{-q \cdot r}{2}$

$M_{tss}(r) := \left[\frac{a^2 \cdot (3 + \nu) \cdot (1 - \nu^2)}{16 \cdot (1 + \nu)} - \frac{(1 - \nu^2) \cdot r^2}{16} - \frac{\nu \cdot (3 + \nu)}{16} \cdot (a^2 - r^2) \right] \cdot q$

$r := -a, -a + .21 \cdot \text{in} .. a$





$$\sigma_{tss}(r) := \frac{Mtss(r) \cdot 6}{t^2} \quad \sigma_{ss}(r) := \frac{Mss(r) \cdot 6}{t^2} \quad \epsilon_{tss}(r) := \frac{\sigma_{tss}(r)}{E} \quad \epsilon_{ss}(r) := \frac{\sigma_{ss}(r)}{E}$$

$$\begin{aligned} \sigma_{ss}(0 \cdot \text{in}) &= 9791.9 \cdot \text{psi} & \sigma_{ss}(a) &= 0 \cdot \text{psi} & \epsilon_{tss}(0 \cdot \text{in}) &= 138 \cdot 10^{-6} & \epsilon_{tss}(a) &= 149 \cdot 10^{-6} \\ \sigma_{tss}(0 \cdot \text{in}) &= 3818.8 \cdot \text{psi} & \sigma_{tss}(a) &= 4118.2 \cdot \text{psi} & \epsilon_{ss}(0 \cdot \text{in}) &= 355 \cdot 10^{-6} & \epsilon_{ss}(a) &= 0 \cdot 10^{-6} \end{aligned}$$

Fixed Edges

$$y_{cfe} := \frac{-a^4}{64 \cdot D} \quad *q \quad y_{cfe} = -6.357 \cdot 10^{-6} \cdot \frac{\text{in}}{\text{psi}} \quad *q \quad y_{cfe}(q) := \frac{-a^4}{64 \cdot D} \cdot q \quad y_{cfe}(q) = -0.0017 \cdot \text{in}$$

$$M_{cfe} := \frac{a^2 \cdot (1 + \nu)}{16} \quad *q \quad M_{cfe} = 3.7 \cdot \text{in}^2 \quad *q \quad M_{cfe}(q) := \frac{a^2 \cdot (1 + \nu)}{16} \cdot q \quad M_{cfe}(q) = 1006.9 \cdot \text{lbf}$$

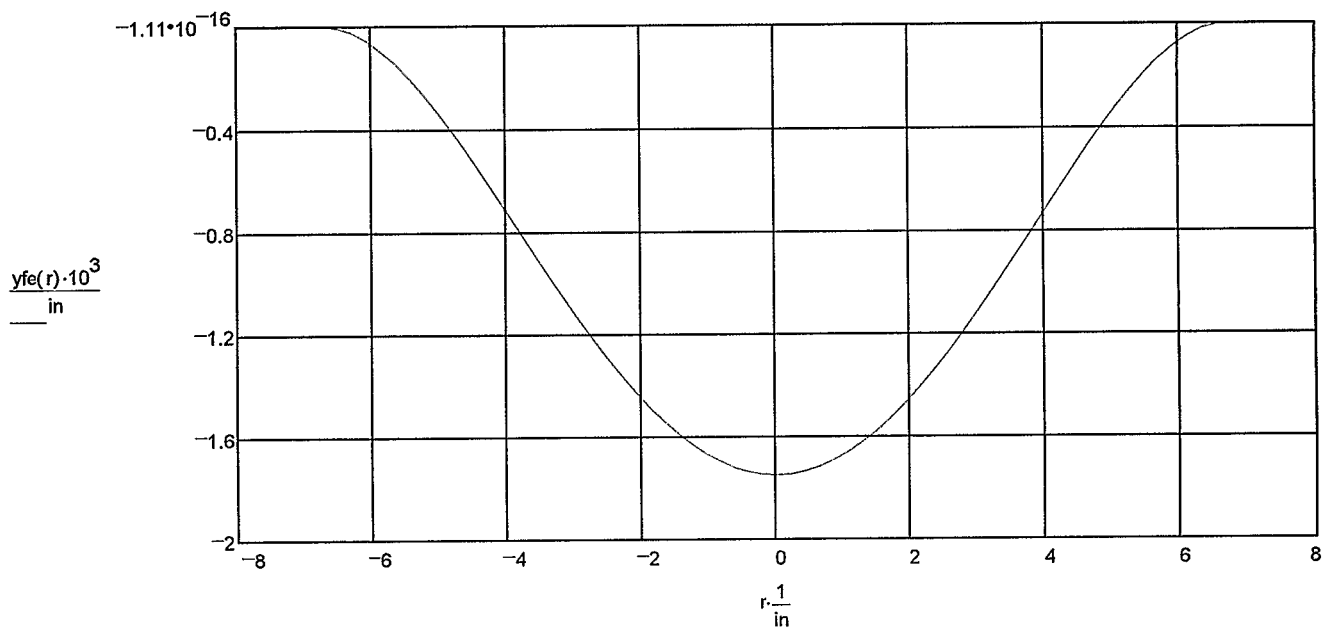
$$\theta_{afe} := 0 \quad *q \quad \theta_{afe} = 0 \quad *q \quad M_{rafe}(q) := \frac{a^2}{8} \cdot -q \quad M_{rafe}(q) = -1543.1 \cdot \text{lbf}$$

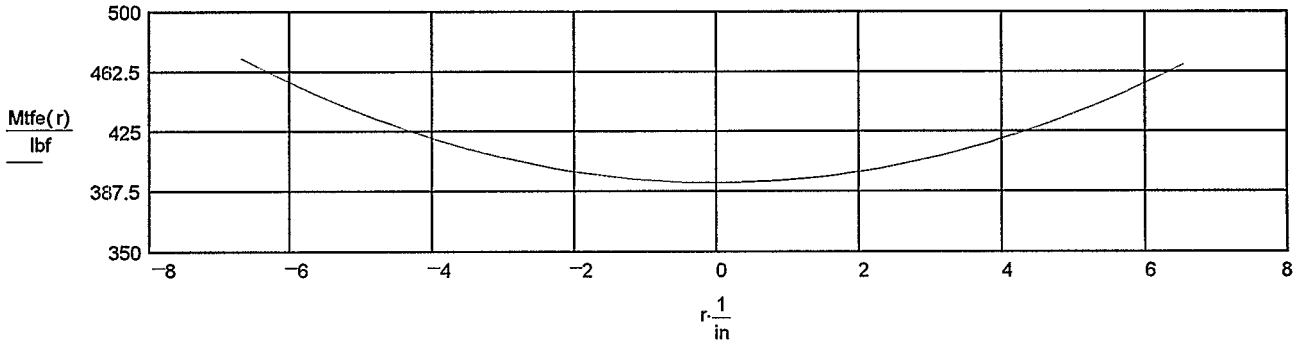
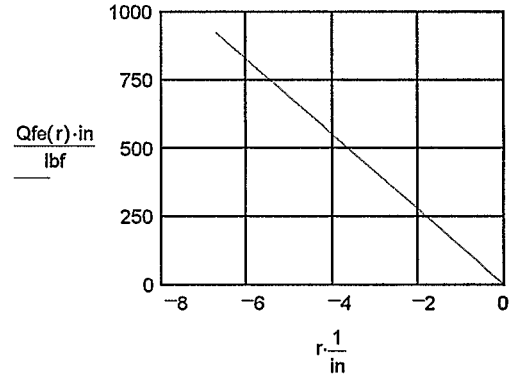
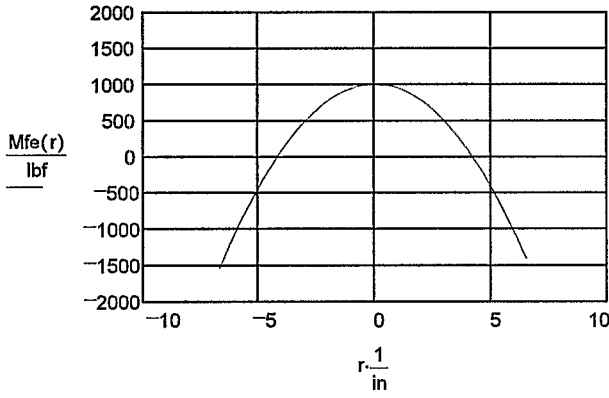
$$Q_{afe} := -\frac{a}{2} \quad *q \quad Q_{afe} = -3.35 \cdot \text{in} \quad *q \quad Q_{afe}(q) := -\frac{a}{2} \cdot q \quad Q_{afe}(q) = -921.25 \cdot \frac{\text{lbf}}{\text{in}}$$

$$y_{fe}(r) := \left(\frac{-a^4}{64 \cdot D} + \frac{a^2 \cdot r^2}{32 \cdot D} - \frac{r^4}{64 \cdot D} \right) \cdot q \quad M_{fe}(r) := \frac{q}{16} \cdot \left[\left[a^2 \cdot (1 + \nu) \right] - \left[r^2 \cdot (3 + \nu) \right] \right] \quad M_{fe}(a) = -1543.1 \cdot \text{lbf}$$

$$M_{tfe}(r) := \left[\frac{a^2 \cdot (1 - \nu^2)}{16} - \frac{(1 - \nu^2) \cdot r^2}{16} - \frac{\nu}{16} \cdot \left[\left[a^2 \cdot (1 + \nu) \right] - \left[r^2 \cdot (3 + \nu) \right] \right] \right] \cdot q \quad Q_{fe}(r) := \frac{-q \cdot r}{2}$$

$$r := -a, -a + .21 \cdot \text{in} .. a$$





$$\sigma_{tfe}(r) := \frac{Mtfe(r) \cdot 6}{t^2} \quad \sigma_{rfe}(r) := \frac{Mfe(r) \cdot 6}{t^2} \quad \epsilon_{tfe}(r) := \frac{\sigma_{tfe}(r)}{E} \quad \epsilon_{rfe}(r) := \frac{\sigma_{rfe}(r)}{E}$$

$$\sigma_{tfe}(0 \cdot \text{in}) = 3866.4 \cdot \text{psi}$$

$$\sigma_{rfe}(a) = -5925.5 \cdot \text{psi}$$

$$\epsilon_{tfe}(0 \cdot \text{in}) = 55 \cdot 10^{-6}$$

$$\epsilon_{tfe}(a) = 65 \cdot 10^{-6}$$

$$\sigma_{tfe}(0 \cdot \text{in}) = 1507.9 \cdot \text{psi}$$

$$\sigma_{rfe}(a) = 1807.3 \cdot \text{psi}$$

$$\epsilon_{rfe}(0 \cdot \text{in}) = 140 \cdot 10^{-6}$$

$$\epsilon_{rfe}(a) = -215 \cdot 10^{-6}$$

$$Q_{fe}(0 \cdot \text{in}) = 0 \cdot \frac{\text{lbf}}{\text{in}}$$

$$Q_{fe}(a) = -921.25 \cdot \frac{\text{lbf}}{\text{in}}$$

Edges with Variable Restraint

$$M_o := -M_{rafe}(q)$$

$$y_{cvr}(q) := \left[\frac{-a^4 \cdot (5 + \nu)}{64 \cdot D \cdot (1 + \nu)} \cdot q \right] + \frac{M_o \cdot a^2}{2 \cdot D \cdot (1 + \nu)} \quad y_{cvr}(q) = 0 \cdot \text{in}$$

$$M_{cvr}(q) := \left[\frac{a^2 \cdot (3 + \nu)}{16} \cdot q \right] - M_o \quad M_{cvr}(q) = 1.007 \cdot 10^3 \cdot \text{lbf}$$

$$\theta_{avr}(q) := \left[\frac{a^3}{8 \cdot D \cdot (1 + \nu)} \cdot q \right] - \frac{M_o \cdot a}{D \cdot (1 + \nu)} \quad \theta_{avr}(q) = 0 \cdot \text{deg}$$

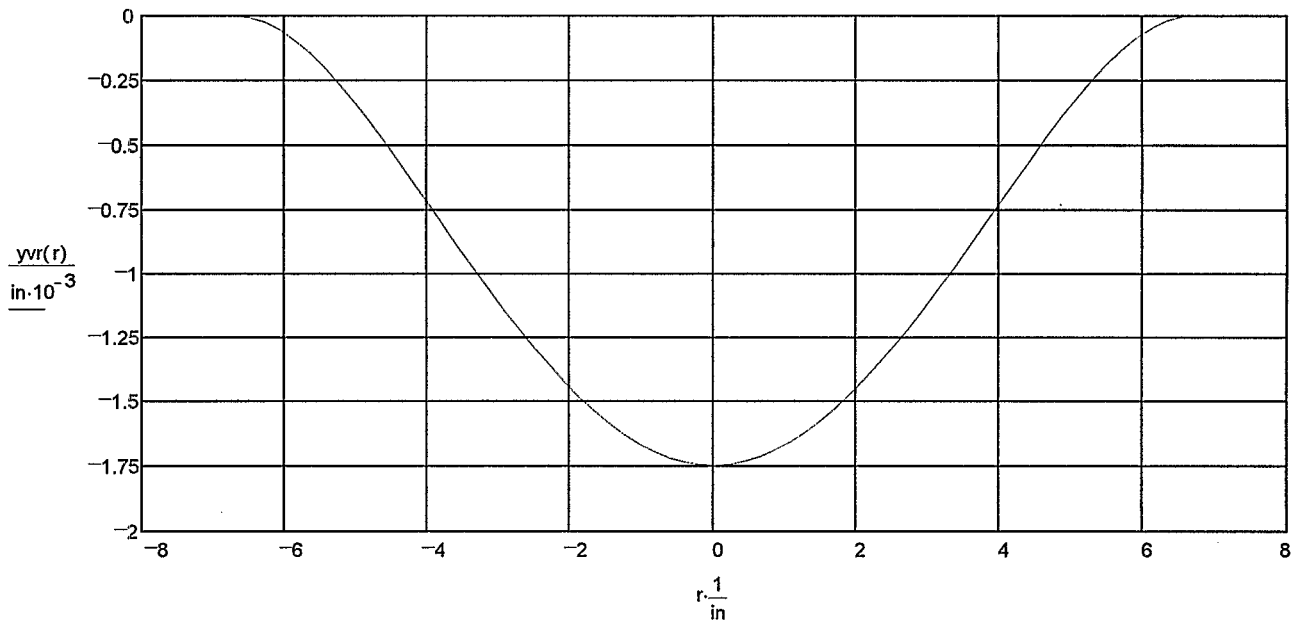
$$Q_{avr}(q) := -\frac{a}{2} \cdot q \quad Q_{avr}(q) = -921.25 \cdot \frac{\text{lbf}}{\text{in}}$$

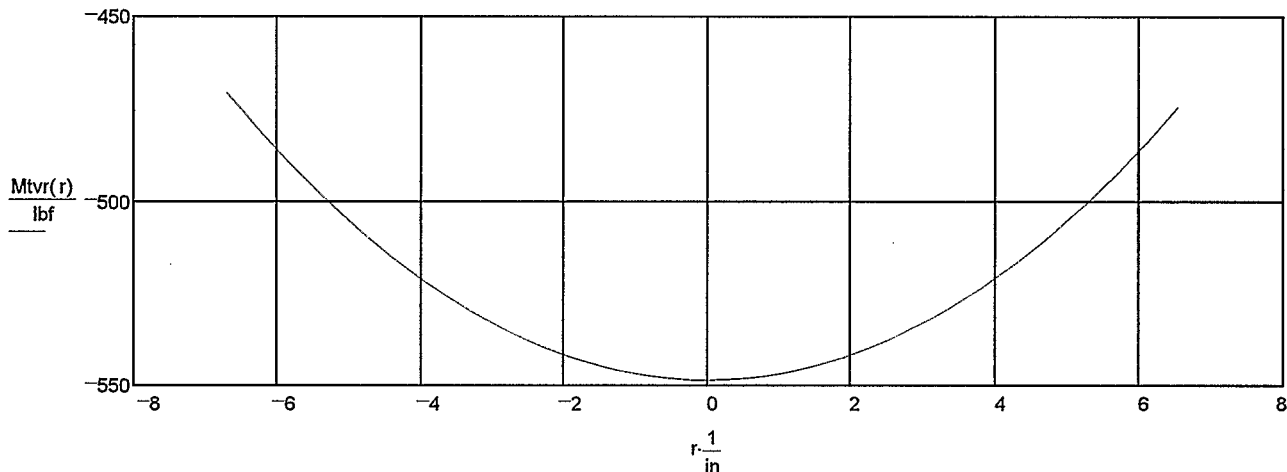
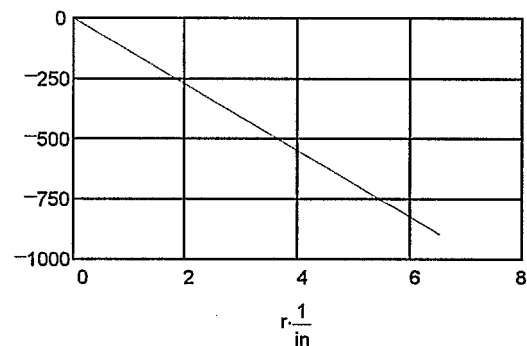
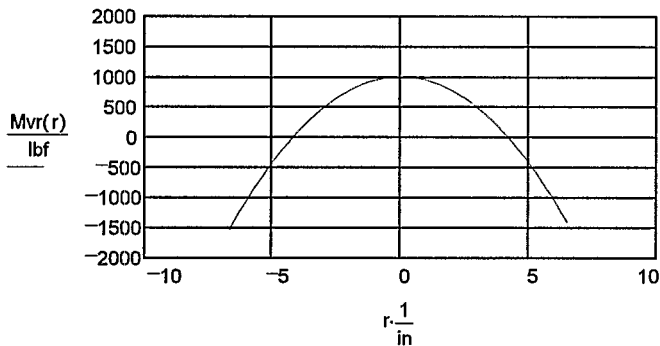
$$y_{vr}(r) := \left[\left[\frac{-a^4 \cdot (5 + \nu)}{64 \cdot D \cdot (1 + \nu)} + \frac{a^2 \cdot (3 + \nu) \cdot r^2}{32 \cdot D \cdot (1 + \nu)} - \frac{r^4}{64 \cdot D} \right] \cdot q \right] + \frac{M_o}{2 \cdot D \cdot (1 + \nu)} \cdot (a^2 - r^2) \quad Q_{vr}(r) := -\frac{q \cdot r}{2}$$

$$M_{vr}(r) := \left[\frac{q \cdot (3 + \nu) \cdot (a^2 - r^2)}{16} \right] - M_o$$

$$M_{tvr}(r) := \left[\left[\frac{a^2 \cdot (3 + \nu) \cdot (1 - \nu^2)}{16 \cdot (1 + \nu)} - \frac{(1 - \nu^2) \cdot r^2}{16} - \frac{\nu \cdot (3 + \nu) \cdot (a^2 - r^2)}{16} \right] \cdot q \right] - M_o \cdot \left[\frac{(1 - \nu^2)}{(1 + \nu)} + \nu \right]$$

$$r := -a, -a + .21 \cdot \text{in} .. a$$





$$\sigma_{vr}(r) := \frac{Mtvr(r) \cdot 6}{t^2} \quad \sigma_{vr}(r) := \frac{Mvr(r) \cdot 6}{t^2} \quad \epsilon_{tvr}(r) := \frac{\sigma_{tvr}(r)}{E} \quad \epsilon_{vr}(r) := \frac{\sigma_{vr}(r)}{E}$$

$$\begin{aligned} \sigma_{vr}(0 \cdot \text{in}) &= 3866.4 \cdot \text{psi} & \sigma_{vr}(a) &= -5925.5 \cdot \text{psi} & \epsilon_{tvr}(0 \cdot \text{in}) &= -76 \cdot 10^{-6} & \epsilon_{tvr}(a) &= -65 \cdot 10^{-6} \\ \sigma_{tvr}(0 \cdot \text{in}) &= -2106.7 \cdot \text{psi} & \sigma_{tvr}(a) &= -1807.3 \cdot \text{psi} & \epsilon_{vr}(0 \cdot \text{in}) &= 140 \cdot 10^{-6} & \epsilon_{vr}(a) &= -215 \cdot 10^{-6} \end{aligned}$$

$$Q_{vr}(0 \cdot \text{in}) = 0 \cdot \frac{\text{lbf}}{\text{in}} \quad Q_{vr}(a) = -921.25 \cdot \frac{\text{lbf}}{\text{in}}$$

$$\begin{aligned} y_{fe}(a - .654 \cdot \text{in}) &= -0.00006 \cdot \text{in} & y_{vr}(a - .654 \cdot \text{in}) &= -0.00006 \cdot \text{in} & y_{ss}(a - .654 \cdot \text{in}) &= -0.00106 \cdot \text{in} \\ y_{fe}(a - .53 \cdot \text{in}) &= -0.00004 \cdot \text{in} & y_{vr}(a - .53 \cdot \text{in}) &= -0.00004 \cdot \text{in} & y_{ss}(a - .53 \cdot \text{in}) &= -0.00085 \cdot \text{in} \\ y_{fe}(a - .4 \cdot \text{in}) &= -0.00002 \cdot \text{in} & y_{vr}(a - .4 \cdot \text{in}) &= -0.00002 \cdot \text{in} & y_{ss}(a - .4 \cdot \text{in}) &= -0.00064 \cdot \text{in} \\ y_{fe}(a - .565 \cdot \text{in}) &= -0.00005 \cdot \text{in} & y_{vr}(a - .565 \cdot \text{in}) &= -0.00005 \cdot \text{in} & y_{ss}(a - .565 \cdot \text{in}) &= -0.00091 \cdot \text{in} \\ y_{fe}(0 \cdot \text{in}) &= -0.00175 \cdot \text{in} & y_{vr}(0 \cdot \text{in}) &= -0.00175 \cdot \text{in} & y_{ss}(0 \cdot \text{in}) &= -0.00711 \cdot \text{in} \end{aligned}$$

